Thermopower measurements of the coupling of phonons to electrons and composite fermions

B. Tieke
Research Institute for Materials, High Field Magnet Laboratory, University of Nijmegen, Toernooiveld, 6525 ED Nijmegen, The Netherlands

R. Fletcher
Physics Department, Queen's University, Kingston, Ontario, Canada K7L 3N6

U. Zeitler and M. Henini
Department of Physics, University of Nottingham, Nottingham NG7 2RD, United Kingdom

J. C. Maan
Research Institute for Materials, High Field Magnet Laboratory, University of Nijmegen, Toernooiveld, 6525 ED Nijmegen, The Netherlands

(Received 23 September 1997)

The thermopower of electrons at zero magnetic field and composite fermions (CF's) at high fields in $GaAs/Ga_{1-x}Al_xAs$ heterojunctions has been measured in the temperature range 0.1–1.2 K. In both cases the data are completely consistent with phonon drag being the only visible contribution. The results have been used to evaluate the phonon-limited mobility of electrons and CF's as a function of temperature. The electron mobility is in good agreement with calculation and with previous results deduced directly from the resistivity, but the CF mobility is not. We have previously reported that the thermopowers at filling factors $\nu=\frac{3}{2}$ and $\frac{1}{2}$ are identical. New data at fields up to 30 T show that this is also true for $\nu=\frac{3}{4}$ and $\frac{1}{4}$. The effect of the substrate crystallographic orientation on phonon drag thermopower is reported. [S0163-1829(98)00828-5]

I. INTRODUCTION

This paper is based on an extensive experimental study of the thermopower of two-dimensional electron gases (2DEG's) in $GaAs/Ga_{1-x}Al_xAs$ heterojunctions in the temperature range $0.1<T<1.2$ K and magnetic fields $0\leqslant B<30$ T. In general there are two contributions to thermopower, diffusion S^d and phonon drag S^g, but our experimental results are completely dominated by S^g. This latter is important because S^g gives direct access to phonon coupling to the 2DEG, and yet is independent of electron-impurity scattering and thus the mobility of the sample. To put this in perspective it is worth examining the relative importance of the various scattering mechanisms for the phonons and the 2DEG. Even in very high mobility samples, say 1000 m^2/V s, the scattering of electrons by phonons contributes only about 1% to the total resistivity at 1 K, and as the temperature is decreased this fraction decreases as T^5 in $GaAs/Ga_{1-x}Al_xAs$ heterojunctions. The phonons in the substrate are equally unaffected by the 2DEG, being overwhelmingly scattered by the sample boundaries at these temperatures. Nevertheless, electron-phonon (e-p) scattering is completely responsible for S^g, and electron-impurity (e-i) scattering is not relevant. The decoupling of e-p scattering from e-i scattering is quite remarkable and makes S^g a subtle but valuable probe. We will use these ideas in the rest of this paper, both at zero field and at high magnetic fields.

This separation of e-p from e-i scattering is the key to the present results so we give a physical picture of how it comes about. An applied temperature gradient ∇T in the substrate leads to a flow of phonons from hotter to cooler regions, and this flow carries a momentum current $\propto -\Lambda\nabla T$, where Λ is the phonon mean free path. A tiny fraction of this momentum current is transferred to the electrons at a rate proportional to $1/\tau_{ep}$, where τ_{ep} is the e-p momentum relaxation time, giving rise to an electric current $\mathbf{j}_{th}$. The magnitude of $\mathbf{j}_{th}$ is also proportional to the time for which the electrons retain the acquired momentum, i.e., to the e-i momentum relaxation time τ_{ei}. (Here we are assuming that $\tau_{ep}\gg\tau_{ei}$.) Thus we have $\mathbf{j}_{th}\propto\tau_{ei}\Lambda\nabla T/\tau_{ep}$, a positive quantity for electrons. The thermopower is measured with no external electric current so an electric field $\mathbf{E}$ is established to provide a compensating current $\mathbf{j}_E=\sigma\mathbf{E}$, where σ is the conductivity $\propto\tau_{ei}$. With $\mathbf{j}_{th}+\mathbf{j}_E=0$ we have $\mathbf{E}\propto-\Lambda\nabla T/\tau_{ep}$. The thermopower S is defined by $\mathbf{E}=S\nabla T$ so we see that $S^g\propto-\Lambda/\tau_{ep}$. The essence of this argument is that the rates of momentum transfer to the 2DEG by $\mathbf{E}$ and phonon coupling are equal and opposite in equilibrium, and neither depends on τ_{ei}. The argument is also valid in a magnetic field, at least semiclassically. A relation embodying these key elements was first derived by Herring[1] for 3D semiconductors, and this is usually written

$$S_0^g=-\frac{\Lambda v}{\mu_{ph}T}, \tag{1}$$

where we use S_0^g to indicate the zero-field value of phonon drag, v is the sound velocity, and μ_{ph} the phonon limited mobility of the electrons $e\tau_{ep}/m^*$, e being the magnitude of the electronic charge and m^* the effective mass of the electrons. The applicability of Eq. (1) to the present work will be examined in more detail later in the paper.

We briefly outline our understanding of the behavior of 2DEG's at high magnetic fields, particularly with respect to S. When the Landau-level filling factor ν takes certain values given by rational fractions with even-integer denominators, the 2DEG is best described as a collection of quasiparticles called composite fermions (CF's), each corresponding to an electron (or hole) associated with an even number, equal to the integer denominator, of flux quanta ϕ_0.[2,3] We are primarily interested in the thermopower of CF's at $\nu=\frac{3}{2}$, $\frac{3}{4}$, $\frac{1}{2}$, and $\frac{1}{4}$, with most of the experimental emphasis being on $\frac{1}{2}$. At these precise values of ν the CF's behave as if the external field is zero and we are able to interpret our data using theories of 2DEG's in zero field, particularly in the case of the thermopower.

We have previously shown[4] that the low-temperature thermopower $S_{xx}(\nu)$ at the fractions $\nu=\frac{3}{2}$, $\frac{3}{4}$, and $\frac{1}{2}$ all have the same temperature dependence ($T^{3.5\pm0.5}$) which within experimental error is the same as that for the 2DEG at zero field ($T^{4.0\pm0.5}$). We also found that $S_{xx}(\frac{3}{2})$ and $S_{xx}(\frac{1}{2})$ were accurately the same at low temperatures. The present work extends the experimental data to $S_{xx}(\frac{1}{4})$, which is found to equal $S_{xx}(\frac{3}{4})$ at low temperatures.

The observed temperature dependence of the thermopower at zero field is that expected[4] for S^g; in this paper we will also show that the absolute magnitude is close to the theoretical estimate. In view of the similar temperature dependence, we have previously concluded that the thermopower of CF's was also due to phonon drag. As further proof of the drag origin for both electrons and CF's, we have extended the experiments to substrates of different crystallographic orientation. It is well known that phonon focusing influences the thermal conductivity of insulating crystals and that these effects depend on the crystal orientation. We expect phonon drag to be modified in a similar manner, and this is indeed observed.

Having demonstrated that phonon drag is responsible for all our results, we will then use a modified form of Eq. (1) to estimate μ_{ph} for both electrons and CF's.

The paper will also explain our experimental techniques in detail. In view of the many results[4,5] that we have obtained in these experiments, it is important to show that our measurements are reliable and accurate.

II. EXPERIMENTAL TECHNIQUES

Suitable techniques for measuring the thermopower of 2DEG's were described by Fletcher *et al.*[6] for the ^{4}He temperature range and above, and further developed by Zeitler *et al.*[7] for the ^{3}He range. The present measurements were made with a ^{3}He/^{4}He dilution refrigerator at fields up to 30 T provided by a hybrid superconducting/Bitter magnet at the University of Nijmegen. The combination of high field and very low temperature requires particular care to reduce eddy current heating and we have solved this problem by using a refrigerator and sample holder that were both made of plastic.[8]

Figure 1 shows the experimental arrangement. The GaAs substrate was indium soldered at one end to a small brass piece, which, in turn, was thermally bonded to plastic supports. Strips of pure, annealed, silver foil were soldered at one end to the brass piece, the other ends being fed into the mixing chamber via a plastic vacuum feedthrough. In the mixing chamber, good thermal contact to the bath was made by bonding the foils to sinters of silver powder. In this way the sample was *in vacuo*, but had one end thermally anchored to the mixture.

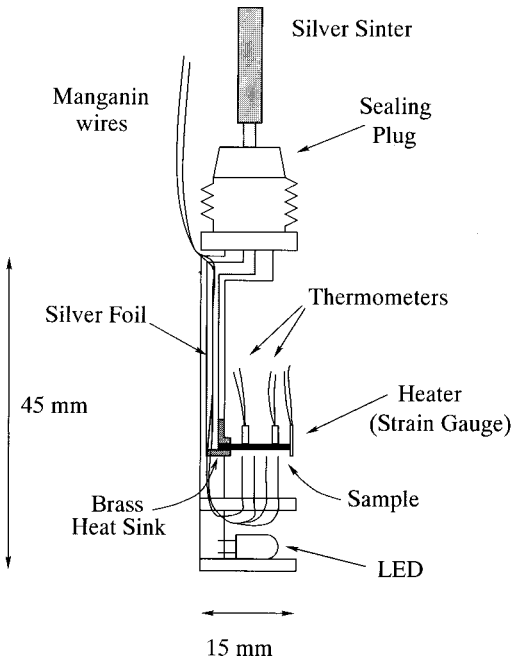

FIG. 1. Sample holder for thermopower measurements. Except for the brass heat sink and the silver foils and sinter, the construction is entirely of plastic.

A small strain gauge acted as a heater and was bonded to the other end of the substrate with epoxy.[9] Two ruthenium oxide chip resistors (Philips 2.21 kΩ), which were found to have negligible magnetoresistance, were used to measure temperature and temperature gradient and were bonded with the same epoxy to the rear surface of the substrate. These were calibrated at zero field by a Speer resistor located in the mixing chamber, which in turn was calibrated by a commercial Ge sensor. The arrangement was usable over the range 0.1–1.2 K. At the highest temperature the refrigerator became unstable and at the lowest the thermoelectric signals become too small to measure.

Twisted pairs of 100-μm-diameter manganin were used for wiring. Manganin gives a very high thermal resistance, but has a negligible thermopower compared to the 2DEG's. The wires were thermally anchored using epoxy[9] at the 1-K pot and also along the silver foils. Plastic disks attached to the bottom of the sample holder provided support for the wiring and also for an infrared diode. Local flexible connections to the ruthenium oxide thermometers were made with 50-μm manganin wires, and to the sample by 25-μm gold wires. In the latter case the gold wires were always in series with manganin wires to provide the necessary thermal isolation of the sample.

Measurements were made with both dc and ac techniques. With dc (mainly used for zero or fixed field) an EM model N11 nanovoltmeter[10] gave a resolution of about 1 nV for thermoelectric voltages. With ac we used a standard low-frequency (5–10 Hz) lock-in voltmeter. A particularly noteworthy feature is the wave form of the excitation of the

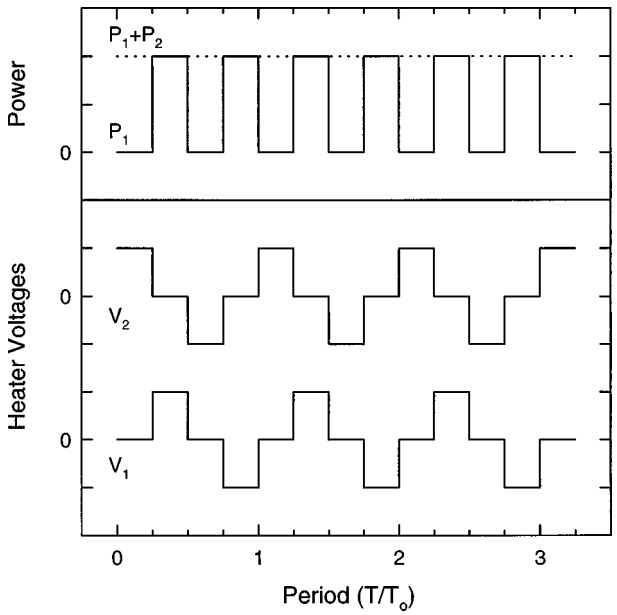

FIG. 2. The voltages V and powers P to the two heaters as a function of time t (in units of the period T_0 of the voltage wave form). The bottom wave form labeled V_1 is the voltage to the sample heater, with the top wave form labeled P_1 giving the resulting power. The middle wave form labeled V_2 is the voltage to the extra heater located on the brass heat sink shown in Fig. 1.

sample heater, which is shown in the lowest curve (labeled V_1) of Fig. 2. The power dissipated in the heater is shown in the top curve (labeled P_1) and, in the ideal case of very fast thermal response, the thermoelectric voltage would follow this wave form; the fundamental of this curve is the thermoelectric component actually measured. Notice that the heater wave form has no frequency component at this frequency. In addition, a second heater located on the brass heat sink was supplied with the same wave form as that to the heater, but phase shifted by $\pi/2$ (middle curve labeled V_2 of Fig. 2). Thus the total heat input to the sample holder was independent of time and the average sample temperature did not cool too much when the sample heater was switched off. In this way rapid thermal equilibrium was achieved and the technique also minimized the effect of any spurious voltages, which are commonly found to occur between any pair of leads in these systems and which are known to be very temperature dependent. Because of this latter advantage, the second heater was also used when measuring at dc to keep the heat into the system constant both with and without a temperature gradient. An analysis shows that the ratio of dc to rms ac voltages is expected to be $\pi/\sqrt{2}=2.22$. In practice the ratio was about 2.7 at 7 Hz due to the finite thermal response time of the system. Finally, the heaters were powered by a voltage generator with an output resistance (including the wiring) matched to the heater resistances. As a result the small changes of heater resistance due to magnetic field caused no significant change in the dissipated power.

For a typical measurement near 500 mK, the temperature could be determined to 1% (giving a possible error in S of 4% because $S \propto T^4$), and the temperature difference of 40 mK to 5%. The error in the thermoelectric voltage (about 400 nV at zero field) was negligible at about 1 nV so that the statistical error in S was $\sim 6-7$ %. At the lowest temperatures, the voltage signals became very small and typically limited the thermopower measurements to $T \geqslant 150$ mK (at $\nu=\frac{1}{2}$ the thermopower is much larger, but the noise was larger by a similar factor). To compare different samples or determine the absolute uncertainty for a particular sample, the possible systematic error in the thermometer spacing and sample contacts must also be included. The former was small at $\sim 2.5\%$ but the latter could be as high as 20%. As a check on the accuracy of the thermometry in a magnetic field we monitored the substrate thermal conductivity but could detect no difference at any field.

III. SAMPLES

The heterojunctions were grown on semi-insulating GaAs substrates at the University of Nottingham. The data presented here were all taken with samples from the same wafer with the 2DEG parallel to the (010) plane. The electron density n and mobility μ could be varied in the range $n=1.0$–1.9×10^{15} m^{-2} and $\mu=60$–100 m^2/V s by illumination from the infrared diode. The data in this paper were all taken at $n=1.75\times10^{15}$ m^{-2}.

Three samples will be discussed. Details of the substrate dimensions and crystallographic orientations are shown in Table I. Samples 1A and 1B were both oriented with their long axis (and ∇T) parallel to [100], and differed only in the width of the central part of the Hall bar (also given in the table). Sample 2 was oriented along [110], but was otherwise nominally the same as sample 1A. Most of the data were taken with 1A and 2. At zero field and for CF's at zero effective field, 1B gave results completely consistent with 1A; more generally there were differences in the thermopowers of these samples at Landau-level peaks, but this is peripheral to the present work and no details will be presented.

The Hall bars were specifically designed for thermopower measurements. Usually the thermopower was measured between the source and drain (the ''current contacts'') which

TABLE I. Geometric details of the three samples. Column 2 gives the dimensions $l_m \times w_m$ of the central part of the Hall bar and column 3 gives the dimensions $l \times w \times t$ of the GaAs substrate. The last columns give the crystallographic orientation of the substrate, the temperature gradient ∇T being parallel to the long axes l and l_m.

Sample	Hall bar mesa $l_m \times w_m$ (mm^3)	Substrate $l \times w \times t$ (mm^3)	Orientation ($\nabla T \| l \| l_m$) l, l_m	w, w_m	t
1A	4.0×0.300	$9.5\times4.0\times0.40$	[100]	[010]	[001]
1B	4.0×0.036	$9.5\times4.0\times0.40$	[100]	[010]	[001]
2	4.0×0.300	$9.5\times4.5\times0.40$	[110]	[$\bar{1}$10]	[001]

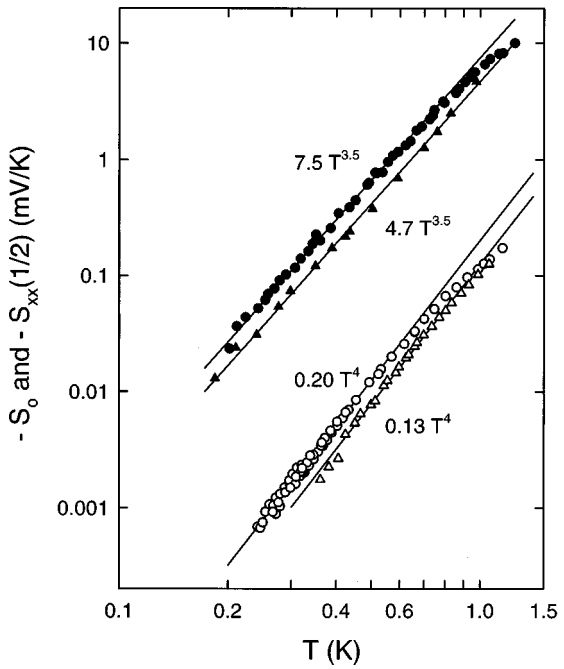

FIG. 3. The open symbols give the thermopower S_0 of the 2DEG's at zero field for the two substrate orientations with the lines being $\propto T^4$. The closed symbols are the thermopower of CF's at $\nu = \frac{1}{2}$, $S_{xx}(\frac{1}{2})$, with the straight lines being $\propto T^{3.5}$. No distinction is made between samples 1*A* and 1*B*, which give indistinguishable curves. In both cases circles correspond to sample 1*A* or 1*B* along [100] and triangles to sample 2 along [110].

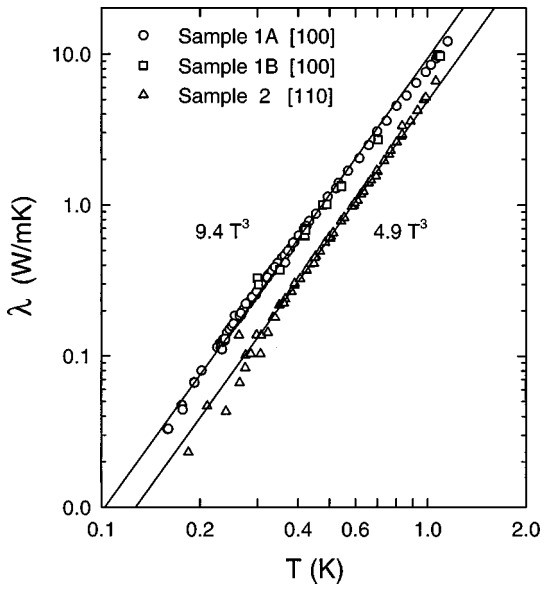

FIG. 4. The thermal conductivity λ for heat flow along different crystallographic directions. The lines show fits to a cubic temperature dependence.

were spaced by 4 mm. Voltage measurements between other pairs of contacts were found to scale accurately with their separation. This was ensured by making contact areas to the sample with small dimensions compared to the sample length.

IV. RESULTS AND DISCUSSION

Zero-field data

Before introducing the results on CF's, we first show that the thermopower at zero field is understood in some detail and is fully consistent with phonon drag. Figure 3 shows the zero-field thermopower S_0 of sample 1*A* ($\nabla T \| [100]$) and sample 2 ($\nabla T \| [110]$). In each case S_0 is strongly temperature dependent and varies as $T^{4.0\pm0.5}$ at low temperatures, as shown by the lines through the data. This temperature dependence is expected for phonon drag as will be shown below. The absolute magnitude of S_0 is not the same for the two samples and we find $S_0(100)/S_0(110) = 1.5_4 \pm 0.3_8$. This difference is attributed to the fact that phonon drag depends on the phonon mean free path Λ, which is different for the two crystallographic orientations because of phonon focusing effects. To our knowledge, this is the first observation of this effect in the thermopower of a 2DEG.

The thermal conductivities of the substrates λ also depend on Λ as demonstrated in Fig. 4. We notice that the data from samples 1*A* and 1*B* are indistinguishable in absolute magnitude perhaps suggesting that our absolute uncertainties may be overestimated. The data have the expected low-temperature behavior $\lambda \propto T^3$ that arises when Λ is a constant determined by boundary scattering. Again we see a difference in absolute magnitudes for differently oriented substrates with $\lambda(100)/\lambda(110) = 1.9_3 \pm 0.3_9$. The ratios for S_0 and λ both contain an uncertainty due to thermometer spacing, but in comparing ratios this error cancels. Not including this error gives $S_0(100)/S_0(110) = 1.54 \pm 0.20$ and $\lambda(100)/\lambda(110) = 1.93 \pm 0.20$. Differences are not unexpected because S_0 and λ are determined by different averages over the phonon spectrum.

An experimental estimate of Λ can be obtained as follows. We can write λ as a sum over the three phonon polarizations i as

$$\lambda = \frac{1}{3}\sum_{i=1}^{3} C_i v_i \Lambda_i = \frac{2\pi^2 k_B^4 T^3}{45\hbar^3} \sum_{i=1}^{3} \frac{\Lambda_i}{v_i^2}, \tag{2}$$

where C_i and v_i are the specific heat and acoustic velocity and the last part of the equation assumes the temperature is low enough that phonon dispersion can be ignored. (The quantities in the sums are actually suitable averages over solid angle for each branch.) Assuming phonon scattering at the surfaces is diffuse and that the phonon spectrum is isotropic, then Λ_i would be constant and the same for each i, say Λ_c. To calculate the v_i we take the low-temperature elastic constants[12] as $c_{11} = 112.6$, $c_{12} = 57.1$, and $c_{44} = 60.0$, all in units of 10^9 N/m^2, and the mass density $\varrho = 5360$ kg/m^3. Then, averaging $\langle 1/v^2 \rangle$ over the three principal symmetry directions [100], [110], and [111], we calculate $\lambda = 3.89\ \Lambda_c T^3$ W/mK. Using the experimental data yields $\Lambda_c = 2.42$ mm for sample 1*A* and $\Lambda_c = 1.26$ mm for Sample 2.

Λ_c can also be independently calculated[11] from the sample dimensions.[11] This predicts $\Lambda_c = 1.06$ mm for sample 1*A* and 1.09 mm for sample 2. However, the elastic anisotropy gives phonon focusing, which affects each branch differently. In GaAs an enhanced average Λ is found for $\nabla T \| [100]$, and a reduced Λ for $\nabla T \| [110]$. The corrections have been calculated by McCurdy[11] and using them we obtain averaged values $\Lambda = 1.39$ mm for sample 1*A* and $\Lambda = 0.83$ mm for sample 2. The experimental values quoted

above are significantly higher than these estimates, presumably due to partial specular reflection, which is always found in samples such as these. The calculated ratio of $\lambda(100)/\lambda(110)=1.67$, which is in reasonable agreement with the experimental ratio of $1.9_3\pm0.20$.

The phonon drag thermopower S_0^g at zero field has been calculated by Cantrell and Butcher[13] and Smith and Butcher.[14] Electrons near the Fermi wave vector $\mathbf{k}_F$ are scattered by phonons of wave vector $\mathbf{Q}=(q,q_z)$ and energy $\hbar\omega_Q$, where q and q_z are the magnitudes of $\mathbf{Q}$ parallel and perpendicular to the plane. The result can be written

$$S_0^g=-\frac{\hbar m^*}{2(2\pi)^3 k_B T^2 n e \varrho}\sum_i \Lambda_i v_i \times\int \Delta(q_z)dq_z\int \frac{E^2 q^3 Q^2 G(Q)}{\epsilon^2(q)}\frac{e^\gamma}{(e^\gamma-1)^2}dq, \quad (3)$$

where $\gamma=\hbar\omega_Q/k_BT$, ϱ is the mass density of GaAs, and E is the deformation potential. The other factors are $\Delta(q_z)=|\int\phi^*(z)e^{iq_zz}\phi(z)dz|^2$, which takes into account the finite thickness of the 2DEG; $\epsilon(q)$ is the static dielectric screening function given by $1+(Q_s/q)F(q)$ (for $q<2k_F$) where $Q_s=2m^*e^2/\kappa\hbar^2$ is the screening wave vector, κ is the dielectric constant of GaAs and $F(q)$ a form factor;[15] $G(Q)=2/[(\hbar^2k_Fq/m^*)^2-\{\hbar\omega_Q-(\hbar^2q^2/2m^*)\}^2]^{1/2}$. The limits of integration are discussed in the references. For GaAs at low temperatures, e-p coupling is dominated by the piezoelectric interaction[15] and E^2 is replaced by[15] $(eh_{12})^2A_l/Q^2$ and $(eh_{12})^2A_t/Q^2$ for longitudinal and transverse modes, where eh_{12} is a piezoelectric constant, and $A_l=9q^4q_z^2/2Q^6$ and $A_t=(8q^2q_z^4+q^6)/4Q^6$ are dimensionless anisotropy factors and each transverse mode is to be counted separately.

Equation (3) considerably simplifies at very low temperatures when $Q\ll2k_F$ and in this limit $G(Q)$ reduces to $2m^*/\hbar^2k_Fq$. In the same limit we take $\Delta(q_z)\to1$, $F(q)\to1$, and $\epsilon(q)\to(Q_s/q)^2$. Finally, using $u=\hbar qv_i/k_BTq$ and $w=\hbar q_zv_i/k_BT$, Eq. (3) can be written in the low-temperature limit as

$$S_0^g=-\frac{m^{*2}(eh_{12})^2k_B^5T^4}{4\pi^2eQ_s^2\hbar^7k_F^3\varrho}\sum_{i=1}^{3}\frac{\Lambda_i}{v_i^5}\int_{-\infty}^{\infty}dw\int_0^\infty a_iu^4\frac{e^\gamma}{(e^\gamma-1)^2}du, \quad (4)$$

where $a_l=9u^4w^2/2(u^2+w^2)^3$ and $a_t=(8u^2w^4+u^6)/4(u^2+w^2)^3$ are the anisotropy factors and $\gamma=\sqrt{u^2+w^2}$. Given that λ has already shown Λ to be independent of T, then $S_0^g\propto T^4$ in excellent agreement with the experimental data.

To evaluate Eq. (4) we take Λ_i to be independent of i and use the average experimental value from λ. Using averaging of $1/v_i^5$ over the same three principal directions as before we find effective velocities of $v_l=5020$ m/s and $v_t=2752$ m/s, and with $h_{12}=1.2\times10^9$ V/m and $\kappa=12.2$ (Ref. 16) we calculate $S_0^g=-0.29T^4$ mV/K for sample 1A and $S_0^g=-0.15T^4$ mV/K for sample 2, which are to be compared with the experimental results of $S_0^g=-0.20\pm0.04T^4$ mV/K and $S_0^g=-0.13\pm0.03T^4$ mV/K, respectively. Given that the calculated values are particularly sensitive to the averaging of the velocities and are subject to errors of $\sim20\%$ from this source alone, the agreement is very satisfactory.

To summarize the discussion so far, the foregoing analysis is completely consistent with phonon drag being the origin of the observed S_0 at low temperatures. The temperature dependence and the absolute magnitudes are accurately predicted by theory, and the substrate orientation dependence is in qualitative accord with expectations. In principle another component of S_0 arises from diffusion, given by

$$S_0^d=-\frac{\pi^2k^2T}{3e\varepsilon_F}(1+p), \quad (5)$$

where ε_F is the Fermi energy and p a constant determined by the energy dependence of the scattering. We see no clear evidence of this contribution in these samples. For $m^*=0.07m_e$ and $n=1.75\times10^{15}$ m^{-2}, then $S_0^d=-4.1T(1+p)$ μV/K, which would roughly double the observed thermopower at 0.3 K if $p=0$, and so be visible. Previous measurements on GaAs heterojunctions have given $p\sim1$, but the absence of S_0^d in our data suggests that p must be negative and ~-1.

As mentioned in the Introduction, S_0^g and μ_{ph} (or $1/\tau_{ep}$) are closely related. In its present form, Eq. (1) is somewhat ambiguous about the appropriate averages for v and Λ, and, in fact, it has usually been treated as a qualitative or semiquantitative relation.[1,17,18] In the following we show that there is a precise version of this equation, at least at low temperatures.

Stormer *et al.*[19] have given explicit results for $1/\tau_{ep}$ in the low-temperature limit [with assumptions equivalent to those with Eq. (4)]. For piezoelectric scattering by longitudinal $(1/\tau_{ph,l})$ and transverse $(1/\tau_{ph,t})$ phonons they find the following:

$$\frac{1}{\tau_{ph,l}}=\frac{63\times5!\zeta(5)}{2^{11}\pi}\frac{m^*(eh_{14})^2(k_BT)^5}{Q_s^2\hbar^7k_F^3\varrho v_l^6}, \quad (6a)$$

$$\frac{1}{\tau_{ph,t}}=\frac{\left(3+\frac{63}{8}\right)\times5!\zeta(5)}{2^9\pi}\frac{m^*(eh_{14})^2(k_BT)^5}{Q_s^2\hbar^7k_F^3\varrho v_t^6}. \quad (6b)$$

The equations have been written in terms of Q_s so that they are more easily compared with Eq. (4). On evaluating Eq. (4) numerically and comparing with Eqs. (6) we find that, to an accuracy of better than 0.1%,

$$S_i^g=-\frac{v_i\Lambda_i}{\mu_{ep,i}T}, \quad (7)$$

where $\mu_{ph,i}=e\tau_{ep,i}/m^*$ and S_i^g are the phonon limited mobility and phonon drag contribution resulting from e-p scattering by phonons of polarization i. (The relevant velocity in the present case is actually $\langle1/v_i^5\rangle/\langle1/v_i^6\rangle$, where the averages are over solid angle, but for our purposes this is sufficiently close to v_i to ignore the difference.) We assume that it is possible to prove Eq. (7) analytically since the numerical agreement between Eqs. (4) and (6) is so exact. This relation can also be inferred from an outline of the calculation of $1/\mu_{ph}$ at low temperatures given by Price.[20] The relevant integral [his Eq. (5)] has the same averaging over the phonon spectrum as Eq. (3) when the latter is approximated to the low-temperature limit. This enables us to deduce that the

result is true regardless of the e-p scattering mechanism, with or without screening. For our purposes the numerical result is sufficiently convincing that we conclude, within the framework of Boltzmann theory, that Eq. (7) is precisely obeyed for the scattering of the 2DEG by each phonon polarization in the low-temperature limit.

In view of the physical argument for S^g given in the Introduction, it seems likely that the relation is more general than the low-temperature limit, but we leave this problem to others for a more thorough investigation.

Thus we find

$$\frac{1}{\mu_{ph}}=\frac{m^*}{e}\sum_{i=1}^{3}\frac{1}{\tau_{ep,i}}=-\sum_{i=1}^{3}\frac{S^g_{0,i}T}{v_i\Lambda_i} \tag{8}$$

to be the generalized form of Eq. (1) that we need, at least at low temperatures. Of course our measurements give only $S^g_0=\Sigma_i S^g_{0,i}$, not the individual $S^g_{0,i}$. Similarly we have only an averaged Λ from λ. To proceed we initially ignore phonon focusing so that Λ_i is the same for each i. Evaluating each of the contributions $S^g_{0,i}$ of Eq. (4) for GaAs shows that the sum of the two transverse modes $2S^g_{0,t}/v_t \approx 40 S^g_{0,l}/v_l$. We see that the contribution from longitudinal mode scattering is very small for the case of GaAs and it is an excellent approximation to write

$$\mu_{ph}=-\frac{v_t\Lambda}{S^g_0 T}, \tag{9}$$

i.e., the original Eq. (1) but with v identified as the transverse acoustic velocity.

We now take Λ to be that determined from λ, i.e., Λ_c. Phonon focusing will not have identical effects on λ and S^g so this is an approximation, but we believe it will not lead to serious error. Using these results for both substrate orientations we plot μ_{ph} in Fig. 5. The result for μ_{ph} should be independent of substrate orientation and our data are reasonably consistent with this expectation. The dashed line is the low-temperature limit $\mu_{ph}=2.3\times10^4 T^{-5}$ m^2/V s calculated using Eq. (6) with our electron density $n=1.75\times10^{15}$ m^{-2} and averaging $1/v_i^6$ over the three principal symmetry directions. Our data follow the predicted variation $\mu_{ph}\propto T^{-5}$ and also agree well in magnitude. We also show data from Kang *et al.*[21] ($n=1.5\times10^{15}$ m^{-2}) which were obtained directly from measurements of the resistivity ρ. To make comparisons at different densities, note that Eq. (6) predicts $\mu_{ph}\propto n^{3/2}$. Thus the ρ data should be about 25% lower than that from S^g_0, but the actual difference is about a factor of 2. We note that e-p scattering contributes only a tiny fraction to the total ρ at these temperatures and in view of this the observed differences are not unreasonable. Stormer *et al.*[19] have also published data on a higher mobility sample with $n=2.2\times10^{15}$ m^{-2}, but the error bars are significantly larger below 1 K and so we do not reproduce those data here.

V. HIGH MAGNETIC FIELD DATA

The majority of our high-field work focused on $S_{xx}(\frac{1}{2})$ as a function of temperature. Figure 3 shows results on the effect of substrate orientation on $S_{xx}(\frac{1}{2})$. Just as with S_0 we see a clear difference in magnitude for the two cases but the slopes are parallel at low temperatures. In each case $S_{xx}(\frac{1}{2})\propto T^{3.5\pm0.5}$. The consistency of the exponent between the two samples suggests that there is a slight but definite difference from the value of 4.0 ± 0.5, which was consistently found at zero field. The observed ratio of the magnitudes for the two crystallographic directions at $\nu=\frac{1}{2}$ is $S_{xx}(100)/S_{xx}(110)=1.60\pm0.21$, which is to be compared with 1.54 ± 0.20 for the zero-field ratio (both ignore the systematic uncertainties in the thermometer spacing). Again we can estimate the contribution from diffusion using Eq. (5). Taking the effective mass for CF's at about a factor of 10 larger than the band mass and recalling that only a single spin direction is relevant, then we estimate $S^d_{xx}(\frac{1}{2})=-20(1+p)T$ μV/K. Assuming $p\leqslant1$, this is small compared to the observed magnitude down to 0.2 K and it is not surprising that we do not see such a contribution.

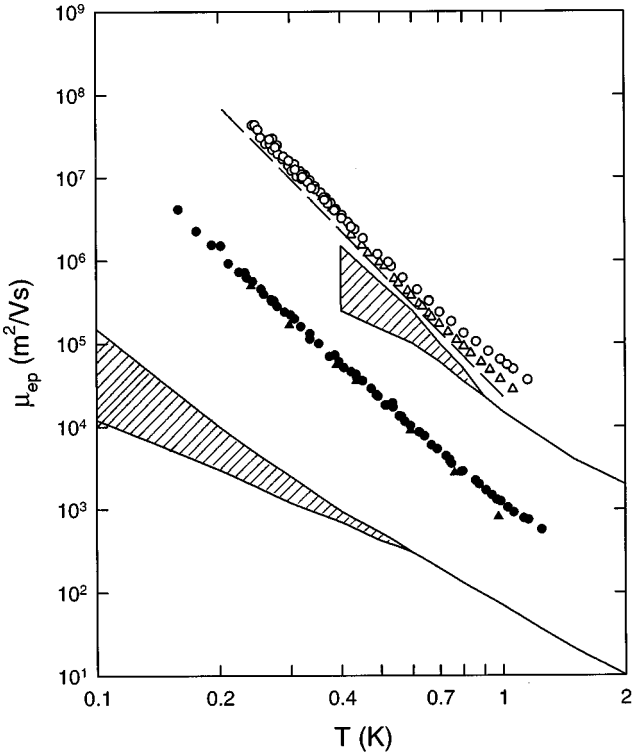

FIG. 5. The open symbols show μ_{ph} for 2DEG's at zero field evaluated from S^g_0 for samples with different crystallographic directions. The closed symbols are similar data on μ_{ph} for CF's at $\nu=\frac{1}{2}$ obtained from $S_{xx}(\frac{1}{2})$. In both cases samples $1A$ and $1B$ are represented by circles, and sample 2 by triangles. The broken line through the zero field data is the calculated curve appropriate to $T\rightarrow0$ and $n=1.75\times10^{15}$ m^{-2}. The solid lines (with crosshatched regions giving an estimate of the scatter on the data) were obtained using ρ and are taken from the literature. The upper line is μ_{ph} for electrons taken from Kang *et al.* (Ref. 21) ($n=1.5\times10^{15}$ m^{-2}); the lower line is for $\mu_{ph}(\frac{1}{2})$ and is also taken from the same reference.

The generally similar behavior shown by S^g_0 and $S_{xx}(\frac{1}{2})$ strongly supports the view that phonon drag is also responsible for the observed thermopower of CF's. The good agreement for the ratios of the thermopowers for the two crystallographic orientations also suggests that CF's have the same sensitivity to Λ as electrons. As we discussed earlier, the measured temperature dependence of T^4 for S^g_0 is due to

screened piezoelectric e-p coupling, and so the implication is that CF's interact with phonons in much the same way, though we should point out that unscreened deformation potential coupling has the same low-temperature T^4 dependence.[4]

The strong experimental support for phonon drag and the similarity shown by CF's to electrons leads us to expect that Eq. (9) will also be valid for CF's and so we use it to calculate their phonon limited mobility μ_{ph}. This gives $\mu_{ph}(\frac{1}{2}) \propto T^{-4.5}$ at $T<0.5$ K, very similar to the result at zero field $\mu_{ph} \propto T^{-5}$, and all the data are shown in Fig. 5. Again, the results for both crystallographic orientations of the substrate are consistent with a single curve. At 0.4 K this curve lies about a factor 60 below that for electrons.

Our mobility curve strongly disagrees with that of Kang *et al.*[21] obtained directly from resistivity data, and also shown in Fig. 5. This study found $\mu_{ph}(\frac{1}{2}) \propto T^{-3}$ with a much smaller magnitude. However, according to their data, CF-p scattering contributes only $\sim 0.1\%$ to the total resistivity at 400 mK, and so the behavior of all other resistivity components must be known very accurately to extract the phonon limited part. In particular, the temperature dependence of the resistivities due to impurities and electron interactions must be precisely accounted for. Clearly the data of Kang *et al.*[21] on $\mu_{ph}(\frac{1}{2})$ and our data on $S^g_{xx}(\frac{1}{2})$ are inconsistent with Eq. (9).

An alternative interpretation of the data may be possible according to the calculation of Khveshchenko and Reizer,[22] which deals with phonon scattering by CF's. This calculation also assumes piezoelectric scattering to be dominant and predicts that the behavior of both $S^g_{xx}(\frac{1}{2})$ and $\mu_{ph}(\frac{1}{2})$ depends on the value of $\overline{q}l$, where $\overline{q}$ is the magnitude of the average phonon wave vector and l is the CF mean free path. In the clean limit, $\overline{q}l>1$, they find $S^g_{xx}(\frac{1}{2}) \propto T^2$ and $\mu^{-1}_{ph}(\frac{1}{2}) \propto T^3$. In this region Eq. (9) should be valid, and the calculated temperature variations are indeed in accord with this. Although the experimental $\mu^{-1}_{ph}(\frac{1}{2})$ does show the expected T dependence,[21] $S^g_{xx}(\frac{1}{2})$ clearly does not. We can estimate $\overline{q}l$ using $\overline{q}=k_B T/\hbar \overline{v}$, where $\overline{v}$ is the average sound velocity ~ 4000 m/s, and the conductivity $\sigma(\frac{1}{2})=e^2 k_{F,cf} l/4\pi\hbar$, where $k_{F,cf}$ is the magnitude of the CF Fermi wave vector, with $k^2_{F,cf}=4\pi n$ in the present case. For our sample this yields the temperature $T_{2,cf}$ at which $\overline{q}l=1$ as 0.15 K, and for the sample of Kang *et al.*,[21] which has a CF mobility of about a factor of 5 higher, $T_{2,cf}=0.03$ K. Thus both samples should be in the clean limit over the whole temperature range.

However, in the dirty limit $\overline{q}l<1$, the calculation predicts that $S^g_{xx}(\frac{1}{2}) \propto T^3$ and $\mu^{-1}_{ph}(\frac{1}{2}) \propto \ln(T_{2,cf}/T)$. [The calculations imply that Eq. (9) is invalid in the dirty limit.] The predicted behavior of $S^g_{xx}(\frac{1}{2})$ is now similar to that observed, but that for $\mu^{-1}_{ph}(\frac{1}{2})$ is not. To obtain consistency with the T dependences of both measured quantities we must assume that the thermopower sample was in the dirty limit, and the mobility sample was in the clean limit. We must also assume that the crossover between clean and dirty limits takes place (probably rather suddenly) in the region of $\overline{q}l \approx 8$, so that the transition occurs at ≈ 1.2 K for the thermopower data, and ≈ 0.24 K for the mobility data, thus making sure that both stay in the appropriate regimes over the range of measurements. This alternative explanation of the results implies that the generally similar temperature dependence shown by S^g_0 and $S_{xx}(\frac{1}{2})$ is somewhat coincidental. Higher mobility thermopower samples would be required to test this interpretation.

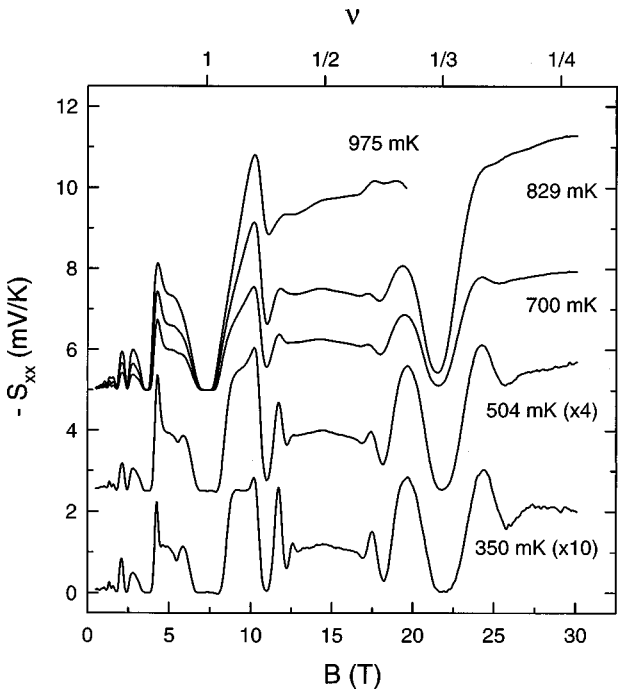

FIG. 6. Examples of the magnetic field dependence of S_{xx} at various temperatures. The curves between 975 mK and 700 mK are offset by 5 mV/K, and that at 504 mK by 2.5 mV/K. Note the scaling factors for the data at the lowest two temperatures.

We have previously published[4] data on S_{xx} as a function of magnetic field to 20 T. These covered the range of filling factor ν down to $\sim \frac{3}{8}$. Figure 6 shows a selection of data that extends the range to 30 T and $\nu<\frac{1}{4}$. We note that, although the resistivity shows a large increase around and beyond $\nu=\frac{1}{4}$ as the system begins to enter the insulating phase at $\nu=\frac{1}{5}$, the thermopower shows no sign of unusual behavior at this point.

In the previous paper[4] we found that $S_{xx}(\frac{3}{2})/S_{xx}(\frac{1}{2}) = 0.99 \pm 0.03$ and $S_{xx}(\frac{3}{4})/S_{xx}(\frac{1}{2}) = 2.15 \pm 0.03$ at $T \leqslant 0.5$ K, even though all these quantities have the same rapid temperature dependence $S_{xx}(\nu) \propto T^{3.5 \pm 0.5}$ (but this dependence is only seen at ν corresponding to CF's). The quasiparticles correspond to electrons attached to $2\phi_0$ for the first two filling factors, and to $4\phi_0$ for the last. Our data at higher field allow us to determine $S_{xx}(\frac{3}{4})/S_{xx}(\frac{1}{4})$ and complete the series. These are shown in Fig. 7, along with $S_{xx}(\frac{3}{2})/S_{xx}(\frac{1}{2})$ for comparison purposes. Although we have much fewer data at $\nu=\frac{1}{4}$, within experimental accuracy, these two ratios have exactly the same temperature dependence and both are unity at low temperatures. We conclude that quasiparticle families with the same denominators (i.e., same number of ϕ_0 attached to each electron or hole) have identical thermopow-

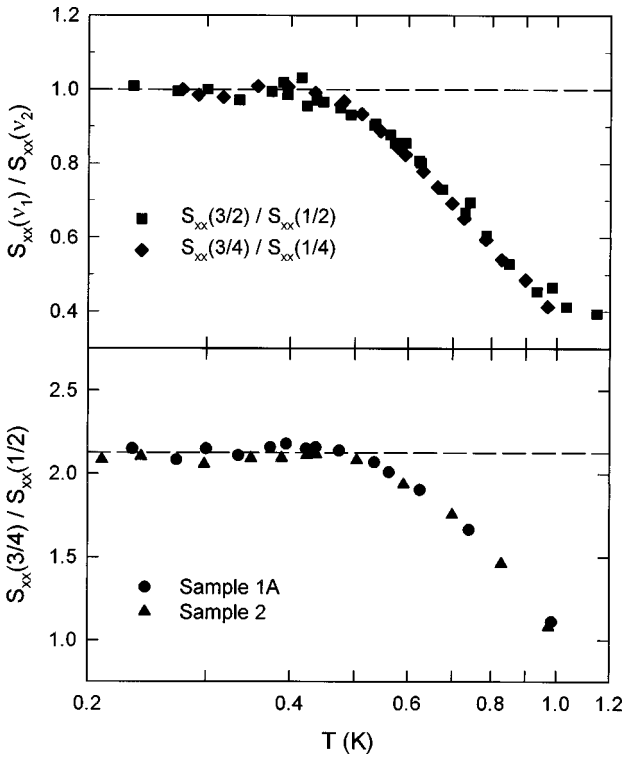

FIG. 7. The upper panel shows the temperature dependence of the ratios $S_{xx}(\frac{3}{2})/S_{xx}(\frac{1}{2})$ and $S_{xx}(\frac{3}{4})/S_{xx}(\frac{1}{4})$. At $T<0.48$ K all the data are consistent with a ratio of unity shown by the dashed line. The lower panel shows the ratio of $S_{xx}(\frac{3}{4})/S_{xx}(\frac{1}{2})$ for the samples 1*A* and 2, which have different substrate orientations. The dashed line is drawn at a ratio of 2.17.

ers. In view of Eq. (9), this implies that μ_{ph} is also the same for each of these families. The lower panel of Fig. 7 shows the ratio of $S_{xx}(\frac{3}{4})/S_{xx}(\frac{1}{2})$ for comparison purposes. At low temperatures this ratio has a value of 2.17, and the temperature dependence is similar to, but not the same as, the ratios in the upper panel.

In the earlier publication[4] we have discussed the possible reasons for the precise equality of $S_{xx}(\frac{3}{2})$ and $S_{xx}(\frac{1}{2})$. In that discussion we assumed that the observed temperature dependence of phonon drag, i.e., T^4, was due to deformation potential scattering without screening [i.e., $\epsilon(q)=1$ in Eq. (3)] for both electrons and CF's. Briefly, the CF states at $\nu=\frac{1}{2}$ and $\frac{3}{2}$ are expected to have the same wave functions, but the latter also has a full Landau level. Thus their electron densities n are the same but the CF densities n_{cf} differ by a factor of 3. Theory shows that the conductivity σ of CF's is enhanced by the factor n/n_{cf}. Our physical model in Sec. I implies that both the current due to CF-p scattering $\mathbf{j}_{th}$ and the compensating current $\mathbf{j}_E$ contain this same factor, which thus cancels in S^g_{xx}. The properties of the CF's still appear in the integral of Eq. (3) through $G(Q)$. We showed that for $G(Q)$ the changes in the factors that depend on CF density, k_F and m^*_{cf}, cancel, so that the overall result is independent of n_{cf} and depends only on n, which is fixed. The one feature that was perhaps unexpected was that one must assume that the effective mass that appears outside the integral in Eq. (3) is the electron mass, whereas naively we would have expected the CF mass to appear here. The extension to the states at $\nu=\frac{1}{4}$ and $\frac{3}{4}$ would follow a similar argument. The latter state is best thought of in terms of holes and their density is again $\frac{1}{3}$ that of the former state.

The present analysis assumes that it is actually screened piezoelectric scattering that is responsible for the observations for electrons. In this case Eq. (4) predicts that at low temperatures phonon drag becomes independent of the effective mass of the electrons because of the factor $Q_s^2 \propto m^{*2}$ in the denominator. This is also true for μ_{ph} through Eq. (6) or Eq. (9). If we assume that the same interaction is still appropriate for CF's and attempt to apply Eq. (4), then we would introduce an extra factor of $Q_s^2 \propto m^{*2}_{cf}$ into the denominator, and we lose the observed equality of S^g_{xx} for CF's with the same denominators. There is certainly doubt in our minds about how screening is accomplished for CF's and what is the appropriate formalism, but we are only able to reproduce the equivalence of the thermopowers at $\nu=\frac{1}{2}$ and $\frac{3}{2}$, and $\nu=\frac{1}{4}$ and $\frac{3}{4}$ by assuming that the effective mass appearing in Q_s is the band mass. Thus we are also unable to understand why S^g and $1/\mu_{ph}$ are both so much larger for CF's than for electrons. In principle the theory of Khveshchenko and Reizer[22] can give a value for the thermopower at different filling fractions but the details are not yet available.

VI. CONCLUSIONS

The experimental results reported in this paper have allowed us to compare the thermopower of 2DEG's in GaAs/$Ga_{1-x}Al_xAs$ heterojunctions at zero field with that of CF's at high magnetic fields. The former have been consistently and convincingly analyzed in terms of phonon drag effects. The theory is based on statically screened, piezoelectric-modulated e-p scattering in the low-temperature limit ($Q \ll 2k_F$) and gives good agreement with experiment in both absolute magnitude and temperature dependence. We have also confirmed that the orientation of the substrate is important in determining the magnitude of the thermopower through phonon focusing effects.

The main features of the thermopower observed for electrons at zero field are reproduced with CF's, i.e., temperature dependence and substrate orientation, though the absolute magnitudes are much higher. These results suggest that the same fundamental processes are responsible in each case, but we are unable to present a framework for understanding the absolute magnitudes in the CF case without making rather *ad hoc* assumptions. The microscopic calculation of the CF-p interaction by Khveshchenko and Reizer[22] is, in principle, capable of consistently reproducing these results, but it is necessary to assume that the thermopower is measured in the dirty limit and the mobility in the clean limit; this requires a rather fortuitous value of the crossover point at which one moves from the clean to the dirty limit to be consistent with all the data.

ACKNOWLEDGMENTS

This work has been supported by the European Commission under Contract No. CHGE-CT93-0051 (Large Installation Plan) and, in part, by the Natural Sciences and Engineering Research Council of Canada.

[1] C. Herring, Phys. Rev. **95**, 1163 (1954).
[2] J. K. Jain, Phys. Rev. Lett. **63**, 199 (1989); Adv. Phys. **41**, 105 (1992).
[3] B. I. Halperin, P. A. Lee, and N. Read, Phys. Rev. B **47**, 7312 (1993).
[4] B. Tieke, U. Zeitler, R. Fletcher, S. A. J. Wiegers, A. K. Geim, J. C. Maan, and M. Henini, Phys. Rev. Lett. **76**, 3630 (1996).
[5] B. Tieke, R. Fletcher, U. Zeitler, A. K. Geim, M. Henini, and J. C. Maan, Phys. Rev. Lett. **78**, 4621 (1997).
[6] R. Fletcher, J. C. Maan, K. Ploog, and G. Weimann, Phys. Rev. B **33**, 7122 (1986).
[7] U. Zeitler, J. C. Maan, P. Wyder, R. Fletcher, C. T. Foxon, and J. J. Harris, Phys. Rev. B **47**, 16 008 (1993).
[8] Hysol epoxy CP4-4285, Dexter Corporation, Olean, New York, NY.
[9] Stycast 2850FT, Emerson and Cuming Inc., Lexington, MA.
[10] EM Electronics, Brockenhurst, England.
[11] A. K. McCurdy, Phys. Rev. B **26**, 6971 (1982).
[12] J. S. Blakemore, J. Appl. Phys. **53**, R123 (1982).
[13] D. G. Cantrell and P. N. Butcher, J. Phys. C **20**, 1985 (1987); **20**, 1993 (1987).
[14] M. J. Smith and P. N. Butcher, J. Phys.: Condens. Matter **1**, 1261 (1989).
[15] S. K. Lyo, Phys. Rev. B **38**, 6345 (1988).
[16] S. Adachi, J. Appl. Phys. **58**, R1 (1985).
[17] R. J. Nicholas, J. Phys. C **18**, L695 (1985).
[18] M. J. Smith and P. N. Butcher, J. Phys.: Condens. Matter **2**, 2375 (1990).
[19] H. L. Stormer, L. N. Pfeiffer, K. W. Baldwin, and K. W. West, Phys. Rev. B **41**, 1278 (1990).
[20] P. J. Price, Solid State Commun. **51**, 607 (1984).
[21] W. Kang, S. He, H. L. Stormer, L. N. Pfeiffer, K. W. Baldwin, and K. W. West, Phys. Rev. Lett. **75**, 4106 (1995).
[22] D. V. Khveshchenko and M. Yu. Reizer, Phys. Rev. Lett. **78**, 3531 (1997).